Supporting Information

Stimuli-responsive "smart probe" for selective monitoring of multiple-cations via differential analyses

Anup Kumar, Alok Kumar Singh and Tarkeshwar Gupta*

Department of Chemistry, University of Delhi, Delhi-110 007, India.

e-mail: tgupta@chemistry.du.ac.in

Material and Methods: Most of the metal salts were purchased from BDH chemicals Ltd. and used as received. 4, 5-imidazoledicarboxylic acid, o-phenylenediamine and ortho-phosphoric acid were purchased from Alfa Aesar and Spectrochem respectively and used as received. $RuCl_3 \cdot \times H_2O$ was purchased from Sigma Adrich and stores in N_2 atmosphere. Methanol, dichloromethane (DCM) and acetonitrile (HPLC grade) were purchased from Merck and distilled using reported methods[S1]. Water used for the experiment was double distilled. UV-Vis spectra were recorded using a JASCO UV-Vis-NIR spectrometer (670D) with a quartz cuvette (path length, 1cm). Fluorescence spectra were recorded on Varian Cary eclipse instrument. IR spectra were recorded on Perkin-Elmer FT-IR spectrophotometer in range 400-4000 cm^{-1} using KBr as a medium. Mass spectra were recorded on THERMO finnigan LCQ advantage max ion trap mass spectrometer (MSAIF, CDRI, Lucknow, India). All ^1H NMR spectra were recorded on Jeol JNMECX 400p spectrometer at room temperature using DMSO-d_6. All chemical shifts (δ) were recorded in ppm with reference to TMS and coupling constant (J) in Hz. X-ray diffraction data for **1** was collected on the Oxford Diffractometer at room temperature equipped with a CCD detector using graphite-monochromated Mo- Kα radiation (λ=0.71073Å). The ligand 4-(1H-benzo[d]imidazol-2-yl)-1H-imidazole-5-carboxylic acid was synthesised by reported synthetic method[S2]. The precursor complex cis-$[Ru(bpy)_2Cl_2].2H_2O$ was prepared according to the reported procedure[S3].

Synthesis of ruthenium complex of 4-(1H-benzo[d]imidazol-2-yl)-1H-imidazole-5-carboxylic acid (1). The initial precursor cis-$[Ru(bpy)_2Cl_2].2H_2O$ (50mg, 0.10 mmol) in dry ethanol (10 ml) was stirred with $AgClO_4$ (54.3mg, 0.26mmol) in nitrogen atmosphere for 30 min. A white colour precipitate was filtered off. Consequently, 4-(1H-benzo[d]imidazol-2-yl)-1H-imidazole-5-carboxylic acid (26 mg, 0.12 mmol) was added to the solution and refluxed for 12h under nitrogen atmosphere. The resulting solution was filtered and dried under vacuo, to yields orange-red colour micro-crystalline solid. The solid product was recrystallized using acetonitrile/methanol (1:2) mixture. Yield: 48 mg (58%). IR (KBr): ν (cm^{-1}) = 1603 (C=O), 1422 (C=N). UV-Vis (CH_3CN; λ, nm); (ε, M^{-1} cm^{-1}): 290 (61,385), 318 (18,860), 354 (14,404), 489 (9645), ES-MS: *m/z* (%): 641(100) [M^+], 526 (22) [$M-C_7H_5N_2$], CV (*vs* Ag/AgCl): $E_{1/2}$ = 0.81 V ($Ru^{2+/3+}$), ΔE = 65.8 mV , Ipc/Ipa = 1.1.

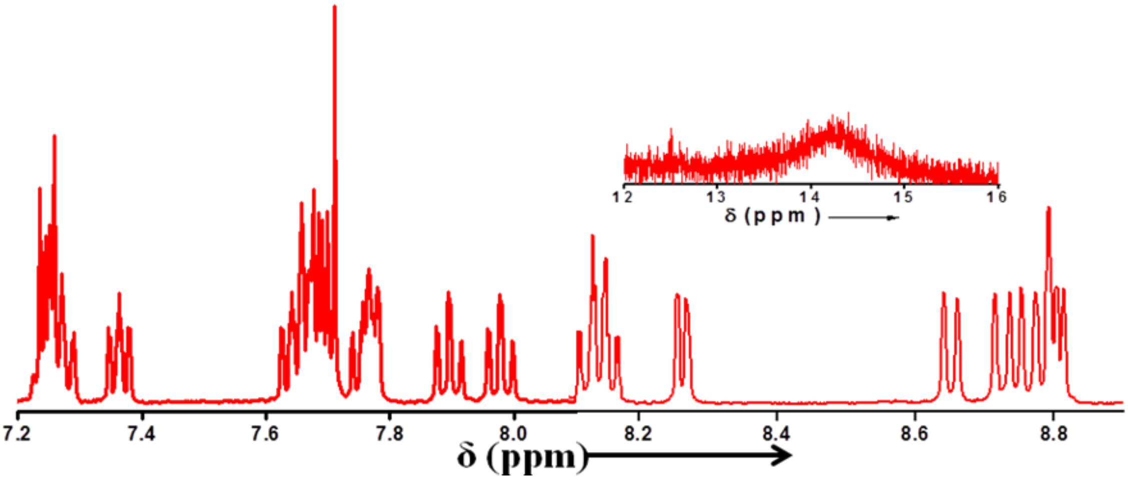

Figure S1: ^1H NMR of **1** in DMSO-d_6 at room temperature, inset highlighting the peak due to the NH proton.

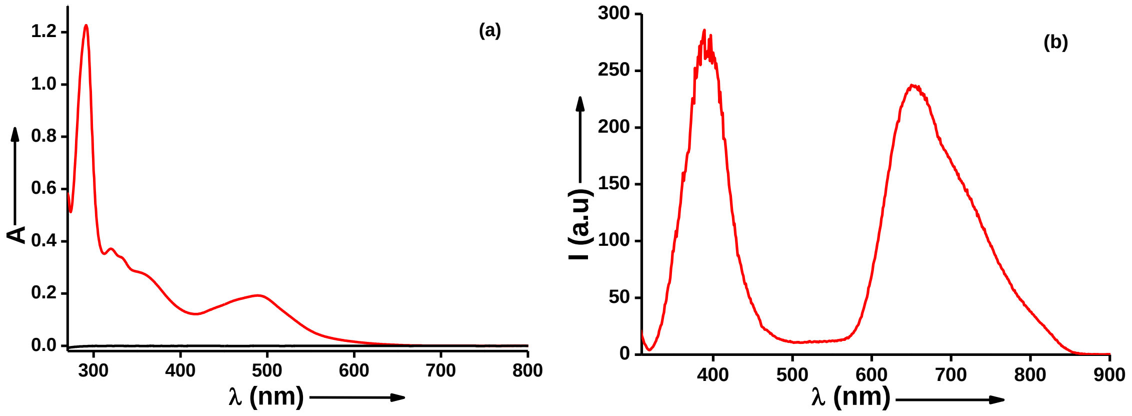

Figure S2: (a) UV-Vis spectra and (b) Emission spectra of **1** (2×10^{-5} M) in acetonitrile at room temperature.

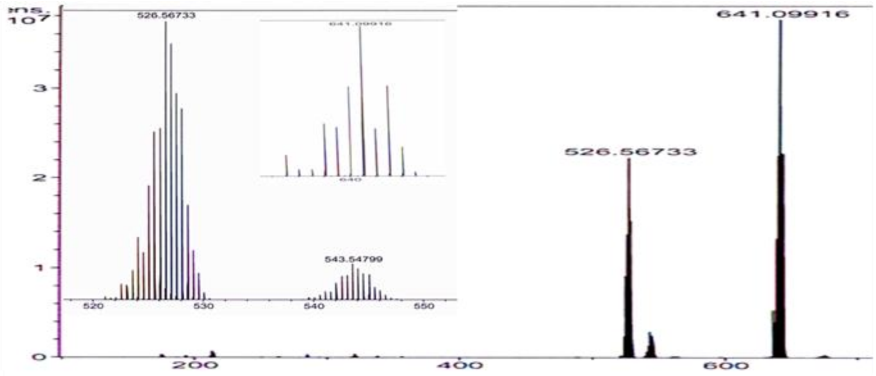

Figure S3: ESI-MS spectra of **1** showing possible fragmentation.

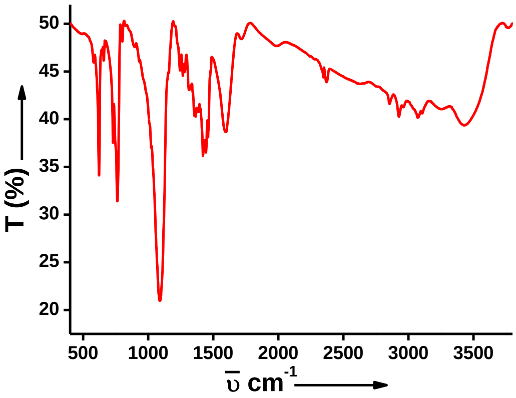

Figure S4: FTIR spectra of **1** in KBr medium.

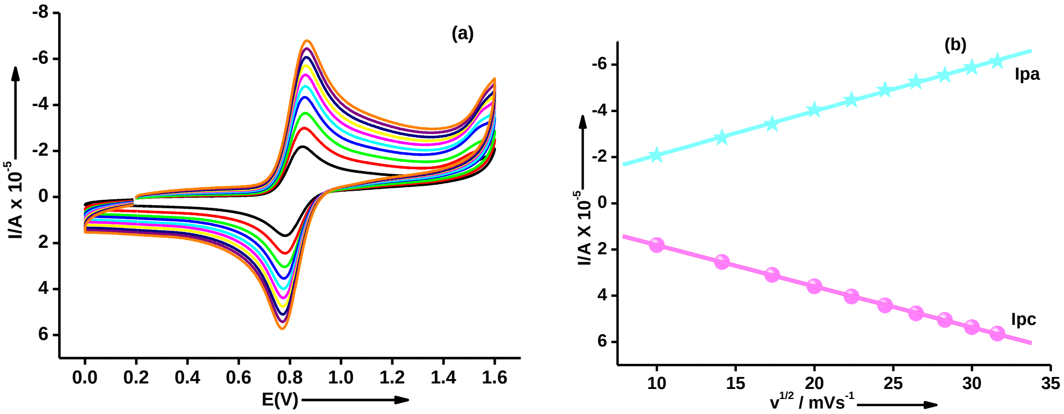

Figure S5: (a) Cyclic voltammogram of **1** (2×10^{-5} M) in acetonitrile containing 1.0 M Bu_4NClO_4 at scan rate from 100 to 1000 mV. The glassy carbon was used as working electrode, platinum wire was used as counter electrode, and Ag/AgCl in 1.0 M KCl aqueous solution was used as reference electrode (b) Plot of current density as a function of scan rate.

Crystallographic Information:

X-ray Crystal structure determination: Crystal suitable for structure determination was obtained by diffusion of diethyl ether over saturated solution of **1** in acetonitrile for one/two week at room temperature. The structure was solved using direct and Fourier methods and refined by full-matrix least squares based on F^2 using WINGX software, which operated SHELX-97 software. The non-H atoms were refined anisotopically. The final least-squares refinement [I >2σ (I)] converged to reasonably good R values, R_1 = 0.0757, wR_2 = 0.2455 for **1**.The goodness of fit for 1.040 and the maximum and minimum peaks on the final difference Fourier map corresponding to 1.443 and -0.688eÅ^{-3} respectively. Complex **1** crystallized in the monoclinic form with space group C2/c.

Selected Bond Angles and Bond lengths:

Selected Bond Angles		Selected Bond Lengths	
N(4)-Ru(1)-N(5)	95.0(2)	O(1)-Ru(1)	2.101(4)
N(4)-Ru(1)-N(6)	96.56(18)	N(2)-Ru(1)	2.060(5)
N(5)-Ru(1)-N(6)	79.26(18)	N(3)-Ru(1)	2.056(5)
N(4)-Ru(1)-N(3)	79.9(2)	N(4)-Ru(1)	2.030(6)
N(5)-Ru(1)-N(3)	100.79(19)	N(5)-Ru(1)	2.034(4)
N(6)-Ru(1)-N(3)	176.4(2)	N(6)-Ru(1)	2.041(4)
N(4)-Ru(1)-N(2)	168.52(17)		
N(5)-Ru(1)-N(2)	95.6(2)		
N(6)-Ru(1)-N(2)	89.80(18)		
N(3)-Ru(1)-N(2)	93.7(2)		
N(4)-Ru(1)-O(1)	90.83(18)		
N(5)-Ru(1)-O(1)	172.01(18)		
N(6)-Ru(1)-O(1)	94.68(16)		
N(3)-Ru(1)-O(1)	85.58(16)		
N(2)-Ru(1)-O(1)	79.10(17)		

Summary of crystal data:

Empirical formula	C62 H48 Cl1 N16 O14 Ru2	
Formula weight	1476.74	
Temperature	298 K	
Wavelength	0.71073 Å	
Crystal system	Monoclinic	
Space group	C 2/c	
Unit cell dimensions	a = 19.9067(8) Å	α= 90°.
	b = 20.3667(6) Å	β= 117.057(5) °
	c= 18.4436(7) Å	γ = 90°.
Volume	6659.3(5) $Å^3$	
Z	4	
Density (calculated)	1.473 Mg/m^3	
Absorption coefficient	0.569 mm^{-1}	
F (000)	2996	
Crystal size	0.22 x 0.16 x 0.14 mm^3	
Theta range	3.19 to 26.00°.	
Index ranges	-23<=h<=24, -25<=k<=25, -22<=l<=22	
Reflections collected	31022	
Independent reflections	6537 [R (int) = 0.0284]	
Completeness to theta = 26.00°	99.8 %	
Absorption correction	Semi-empirical from equivalents	
Max. And min. transmission	0.9244 and 0.8848	
Refinement method	Full-matrix least-squares on F^2	
Data / restraints / parameters	6537 / 0 / 439	
Goodness-of-fit on F^2	1.040	
Final R indices [I > 2 sigma (I)]	R_1 = 0.0757, wR_2 = 0.2455	
R indices (all data)	R_1 = 0.0950, wR_2 = 0.2364	
Largest diff. peak and hole	1.443 and -0.688 $eÅ^{-3}$	
[a]R_1 (F) = $[\sum\|\|F_0\|-\|F_c\|\|/\sum\|F_0\|]$.	[b]wR_2 $(F^2) = [\sum w (F_0^2-F_c^2)^2/\sum w (F_0^2)^2]^{1/2}$.	

Preparation of ppm-level solution of metal salts. A stock solution of 1000 ppm of various metal salts of $Hg(NO_3)_2.H_2O$, $Ni(NO_3)_2.6H_2O$, $MnCl_2.4H_2O$, $MgSO_4$.7H2O, $AgNO_3$, KNO_3, $FeCl_3$, $Cu(NO_3)_2.3H_2O$, $Co(NO_3)_2.6H_2O$, $Cd(NO_3)_2.4H_2O$, LiCl, $CaCl_2$, $Pb(NO_3)_2$, $Zn(NO_3)_2.6H_2O$ and $FeSO_4.7H_2O$ in dry acetonitrile/DMF/DCM were made by dissolving 10 mg of each metal salts in 10 ml of mixture of solvent. Further, the stock solution was diluted to 10 ppm by taking 50ul volume of stock solution (1000 ppm) and making up it in acetonitrile solution of **1** upto 5 ml. The solution was used for analyses.

Detection procedure of ppm-levels of Pb^{2+}, Zn^{2+} and Fe^{2+}: A 5 ml solution of **1** (2×10^{-5}M) was treated with 5ul stock solution (1000 ppm) of Pb^{2+}/Zn^{2+}(1.0 ppm in acetonitrile solution of **1**), mixed thoroughly, allowed to keep undisturbed for 3 minutes. Subsequently, emission spectra were recorded at room temperature using quartz cuvette. Further, 5 ul of Pb^{2+}/Zn^{2+} was added to same solution for 2, 3, 4, 5, 6, 7, 8, 9, and 10 ppm. In Contrast, the ppm levels of Fe^{2+} was retained by addition of 50 ul of stock solution (1000 ppm) of Fe^{2+} in 5 ml of **1** (2 × 10^{-5}M) for 10 ppm and similarly higher concentration was maintained for analyses. The output signal was monitored w.r.t intensity of **1** at both bands.

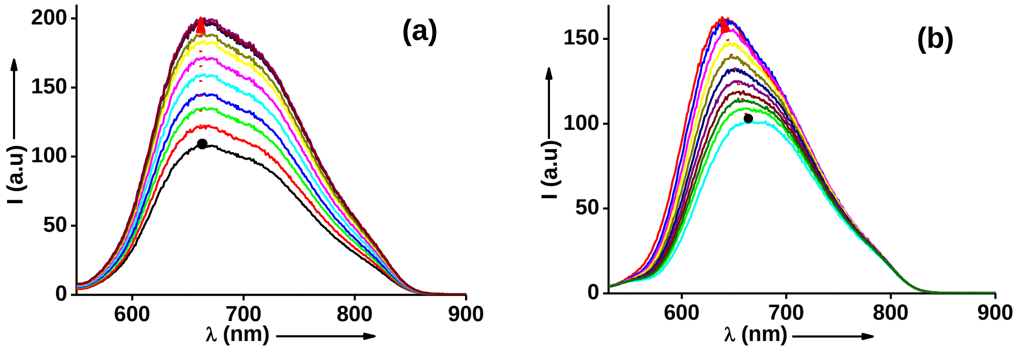

Figure S6: Emission intensity changes of **1** (2 × 10^{-5} M in acetonitrile) upon addition of 1, 2, 3, 4, 5, 6, 7, 8, 9, 10 ppm of Pb^{2+} (a)/Zn^{2+} (b). The spectra were recorded after excitation at 489 nm.

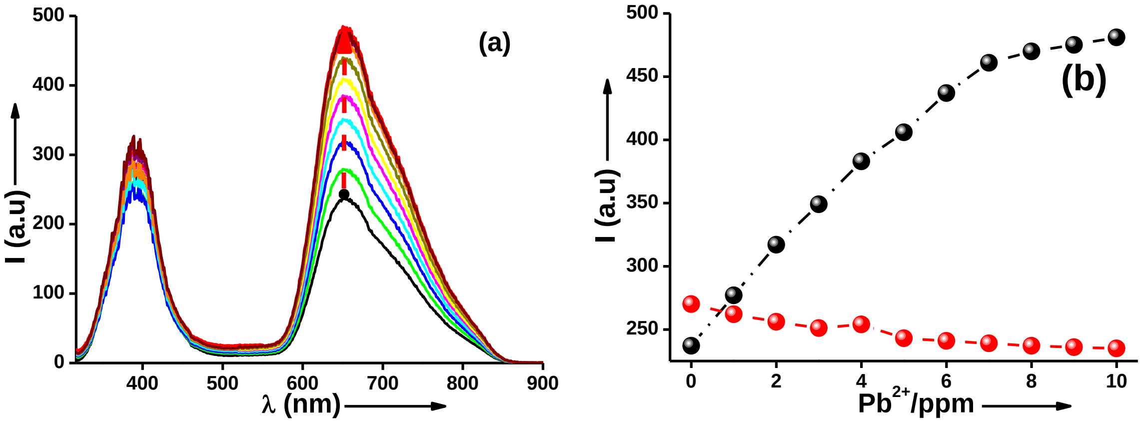

Figure S7: Emission intensity changes of **1** (2 × 10^{-5} M in acetonitrile) upon addition of 1, 2, 3, 4, 5, 6, 7, 8, 9, 10 ppm of Pb^{2+}. The spectra were recorded after 3 min reaction time (a), Plot of emission intensity changes vs. concentration of Pb^{2+} at λ = 655 (black balls) and 389 nm (red star) (b).

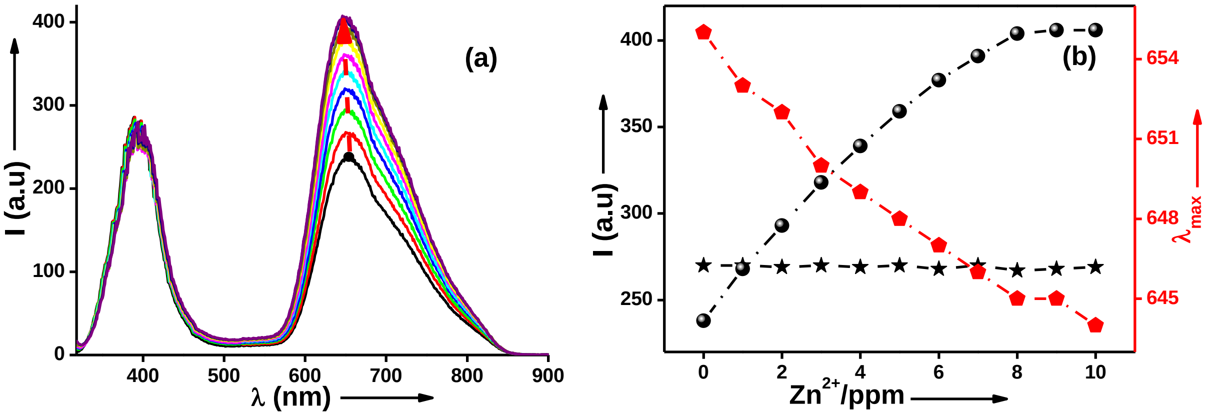

Figure S8: Emission intensity changes of **1** (2×10^{-5} M in acetonitrile) upon addition of 1, 2, 3, 4, 5, 6, 7, 8, 9, 10 ppm of Zn^{2+}. The spectra were recorded after 3 min reaction time (a), Plot of intensity changes vs. concentration of Zn^{2+} at λ = 655 (black balls) and 389 nm (red star).

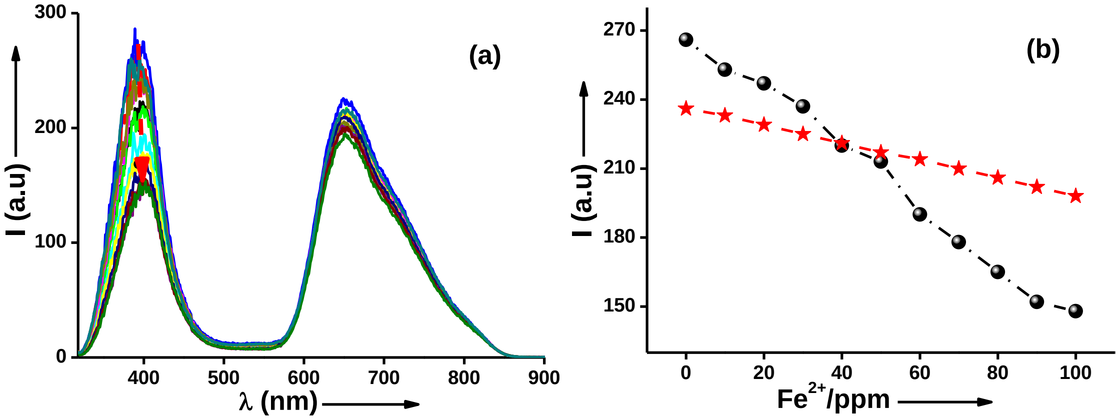

Figure S9: Emission intensity changes of **1** (2×10^{-5} M in acetonitrile) upon addition of 1, 2, 3, 4, 5, 6, 7, 8, 9, 10 ppm of Fe^{2+}. The spectra were recorded after 3 min reaction time (a). Plot of emission intensity changes *vs*. concentration of Fe^{2+} at λ = 655 (red star) and 389 nm (black balls) (b).

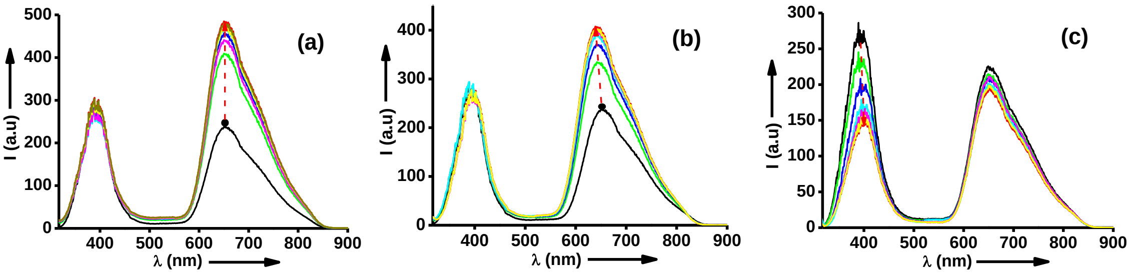

Figure S10: Emission intensity change of **1** (2×10^{-5} M in acetonitrile) as a function of time upon addition of 10 ppm of Pb^{2+} (a) 10 ppm of Zn^{2+} (b) 100 ppm of Fe^{2+} (c).The spectra was taken after 30 sec in each experiment and saturation was achieved within ~3 min.

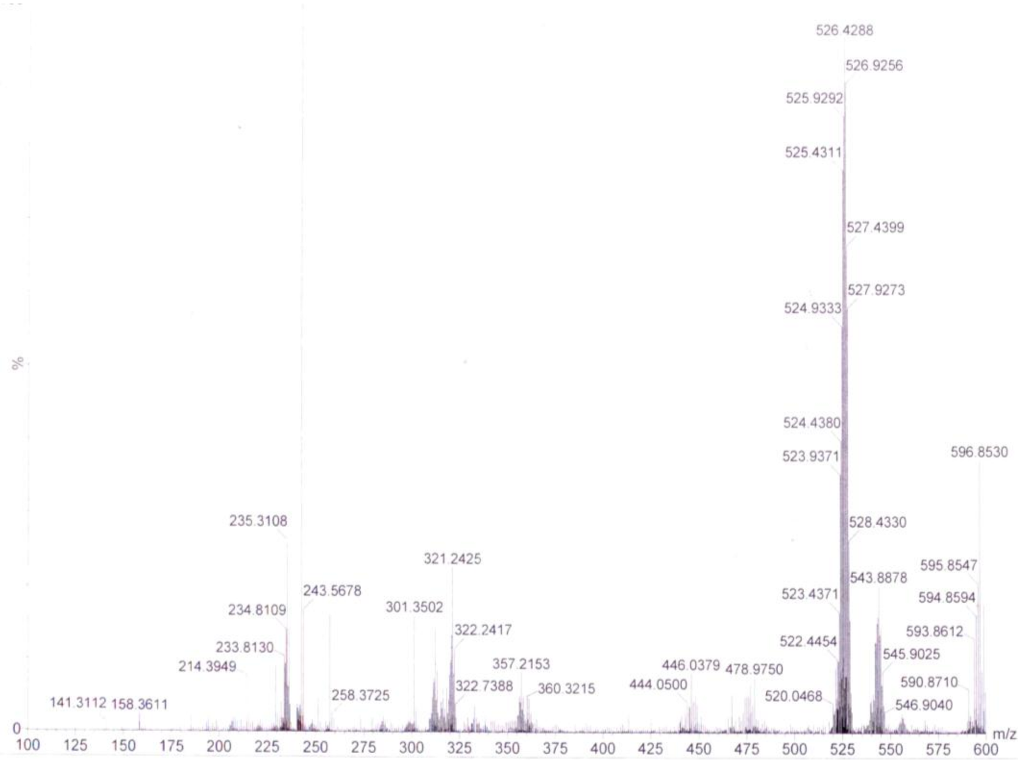

Figure S11: ESI-MS spectra of **1+ Pb^{2+} + Zn^{2+}** showing possible fragmentation.

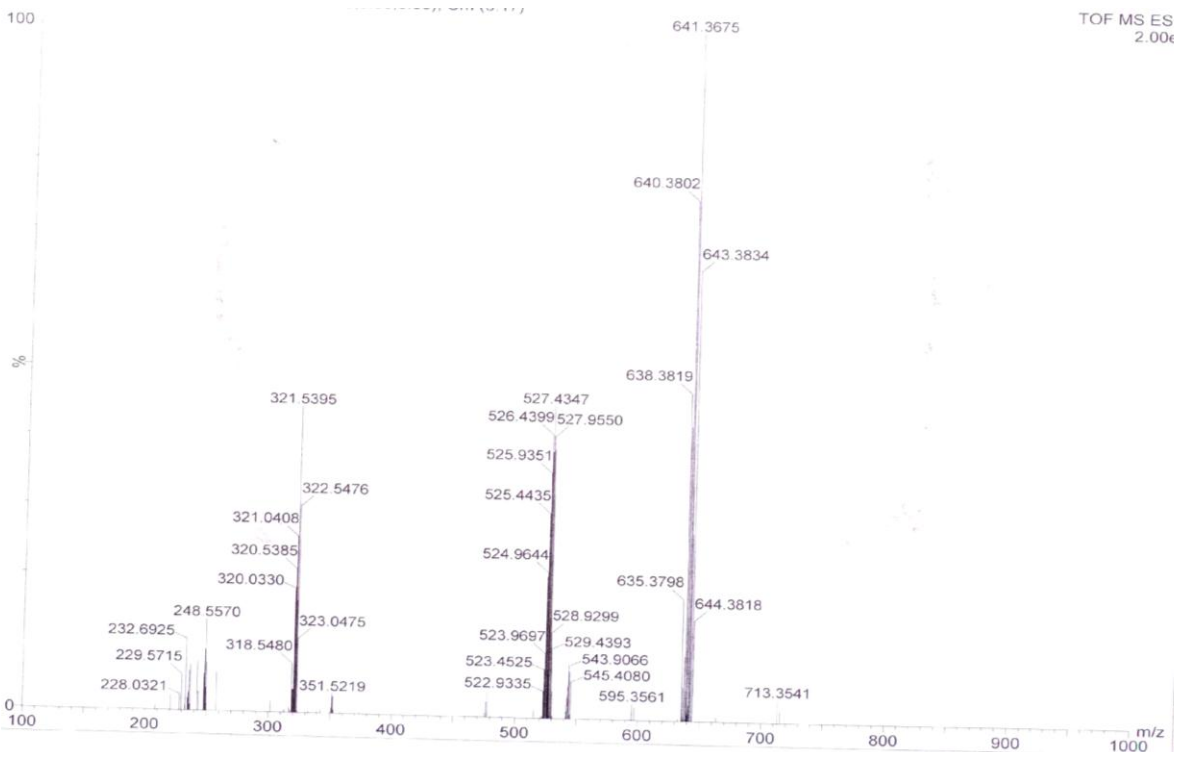

Figure S12: ESI-MS spectra of **1+ Pb**$^{2+}$ **+ Fe**$^{2+}$ showing possible fragmentation.

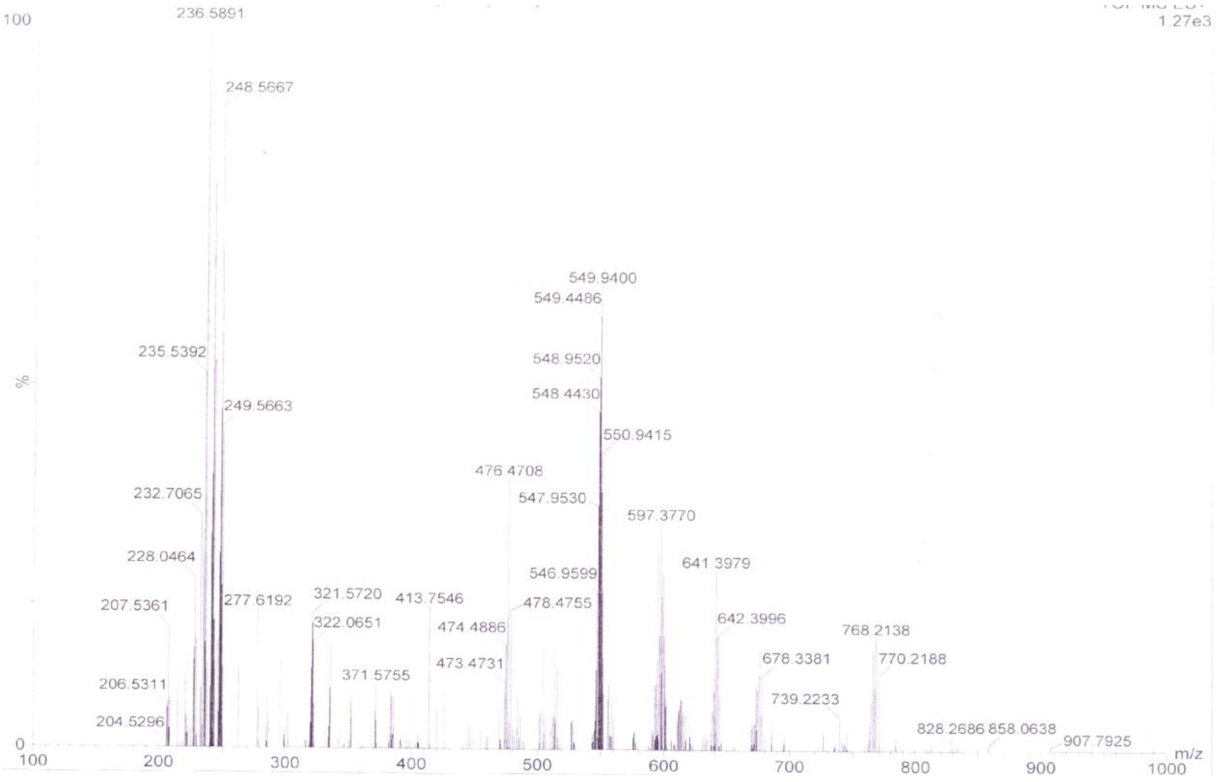

Figure S13: ESI-MS spectra of **1+ Zn**$^{2+}$ **+ Fe**$^{2+}$ showing possible fragmentation.

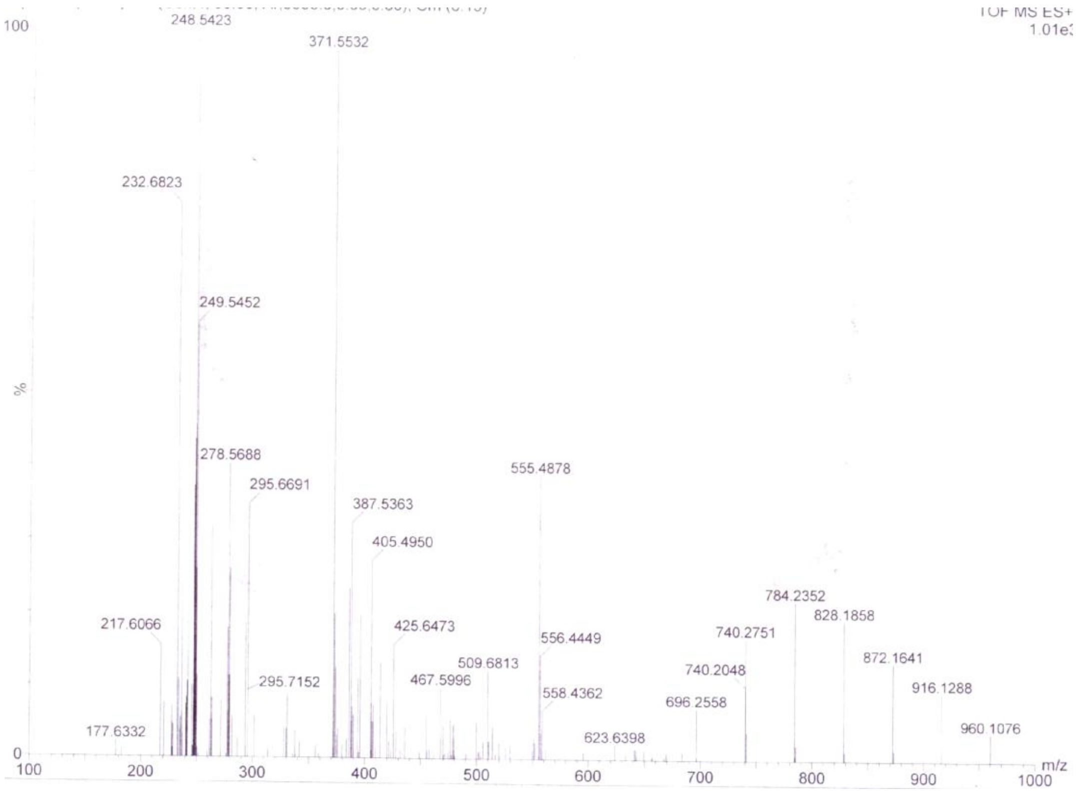

Figure S14: ESI-MS spectra of **1**+ **Pb^{2+} + Zn^{2+} + Fe^{2+}** showing possible fragmentation.

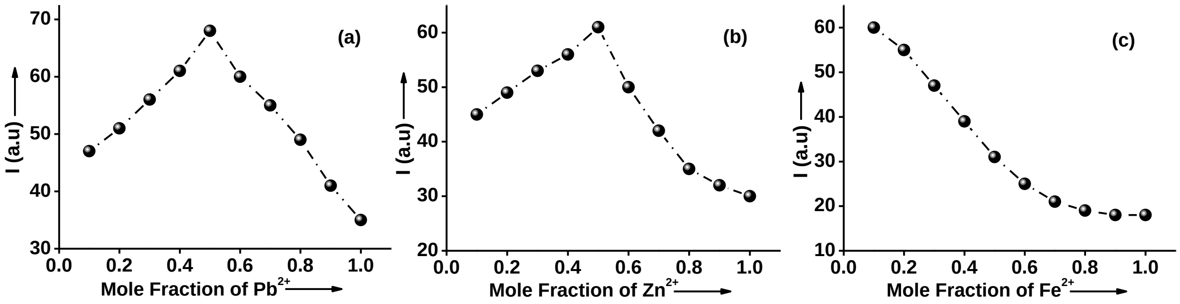

Figure S15: Job's plot for varying mole-fraction of metal-cations (1×10^{-6} M) in **1**(1×10^{-6} M in acetonitrile) Pb^{2+} (a), Zn^{2+} (b), and Zn^{2+} (c).

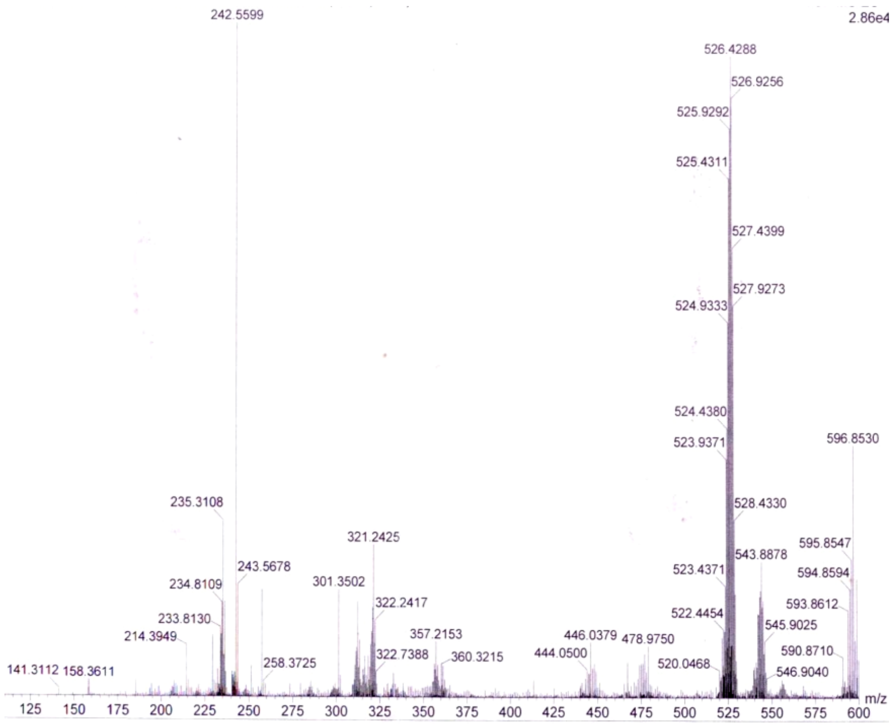

Figure S16: ESI-MS spectra of **1+ Pb**$^{2+}$ showing possible fragmentation.

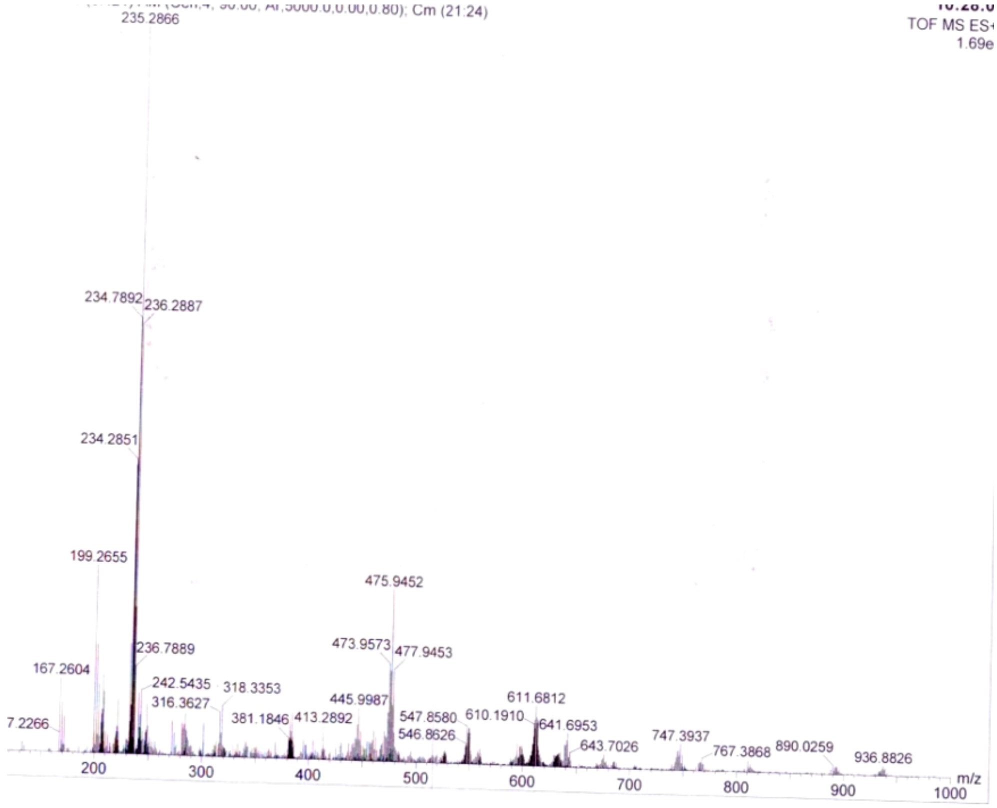

Figure S17: ESI-MS spectra of **1+ Zn**$^{2+}$ showing possible fragmentation.

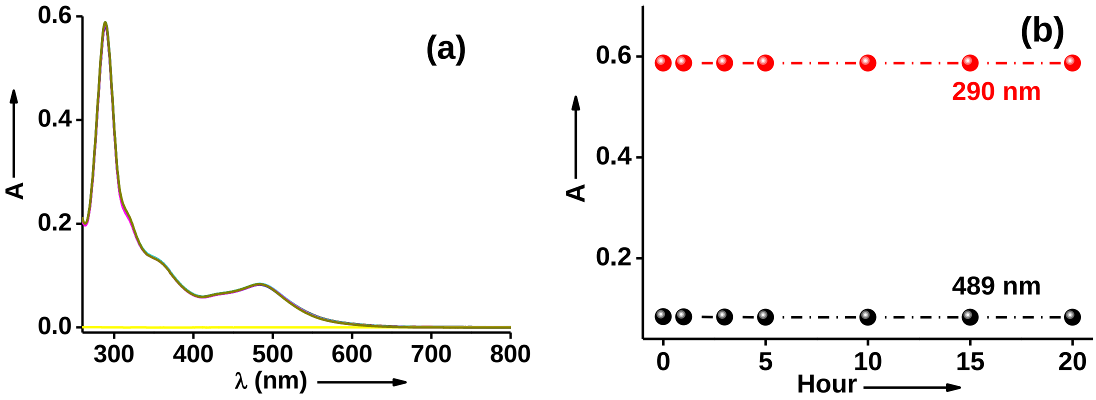

Figure S18: Representative UV-Vis spectra of **1** (0.85×10^{-5}M in CH_3CN) after exposing with sunlight for 20 hour (29 Nov. 2012, temp. 20-27^{0}C, India).

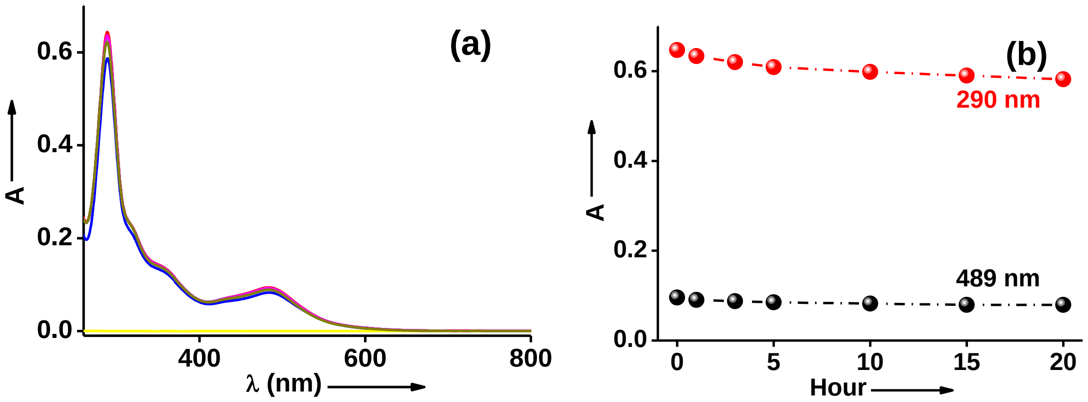

Figure S19: Representative UV-Vis spectra of **1** (0.85×10^{-5}M in CH_3CN) after exposing with UV-radiation for 20 hour (15 W, 356 nm).